

# Structural Modifications of DMPC Vesicles upon Interaction with Poly(amidoamine) Dendrimers Studied by CW-Electron Paramagnetic Resonance and Electron Spin–Echo Techniques

M. Francesca Ottaviani\* and Roberto Daddi

*Department of Chemistry, University of Florence, Via G. Capponi 9, 50121 Firenze, Italy*

Marina Brustolon

*Department of Physical Chemistry, University of Padua, Via Loredan 2, 35131 Padova, Italy*

Nicholas J. Turro

*Department of Chemistry, Columbia University, New York, New York 10027*

Donald A. Tomalia

*Michigan Molecular Institute, Midland, Michigan 48640*

*Received March 16, 1998. In Final Form: September 16, 1998*

This report describes a computer-aided CW- and pulsed-electron paramagnetic resonance (EPR) investigation on the structural modification of dimyristoylphosphatidylcholine (DMPC) vesicles, which occur upon interaction with starburst dendrimers (SBDs). Probes used for this study included doxyl-functionalized stearic acids, with the doxyl group attached at different positions of the stearic chain (5DXSA, 12DXSA, and 16DXSA). Mainly mobility and polarity parameters were evaluated from the analysis of the CW-EPR spectra, whereas the analysis of the decay and modulation of the electron spin–echo (ESE) signal provided information on the structural environment of the paramagnetic center. Due to the interaction with the SBD surface, the vesicle structure became more rigid and ordered. The enhanced rigidity of the structure also caused the tilting of the chains of about 50° with respect to the surface line. The permeability of water at the chain beginning level increased, thus increasing the rotational mobility of the probe. The perturbing effects lessened toward the end of the chains. A fraction of 16DXSA (15%) was in the bent conformation, with the chain inserted into the lipid layer and the two polar heads at the external surface. The interaction with protonated dendrimers caused the swelling of the vesicle structure. This study indicated that the bilayer structure is modified but only partially perturbed by the addition of the dendrimers, and the integrity of the vesicle, as a model cell membrane, is preserved after the interaction with the dendrimers. This is encouraging for the use of the SBDs as drug and gene carriers.

## Introduction

The dendritic macromolecules<sup>1,2</sup> designated starburst dendrimers,<sup>2</sup> which are derived from  $\beta$ -alanine units emanating from a central ethylenediamine core (these dendrimers are termed *n*SBDs, where *n* indicates the generation, that is, the number of concentric layers of  $\beta$ -alanine units), have been shown to function as effective drug delivery agents as carriers for antisense oligonucleotides, and gene expression plasmids for targeted gene

expression.<sup>3,4</sup> When the drug or genetic material is being chaperoned to a target cell, one of the main questions in this process is the possible interaction of the dendrimer with the cell membrane and the eventual modification of the membrane structure.

To investigate interactions occurring between *n*SBDs and the cell membrane, we have recently<sup>5</sup> analyzed the continuous wave (CW)- and pulsed-electron paramagnetic resonance (EPR) spectra of spin-labeled *n*SBDs in the presence of phosphatidylcholine curved bilayers or multilayers, termed vesicles and liposomes.<sup>6,7</sup> These prototypes are widely used as model membranes.<sup>8–10</sup> The SBDs undergo fast exchange between the vesicle surface and

\* To whom correspondence should be addressed.

(1) (a) *Advances in Dendritic Macromolecules*; Newkome, G. R., Ed.; JAI Press: Greenwich, CT, 1993. (b) Newkome, G. R.; Moorefield, C. N.; Baker, G. R.; Johnson, A. L.; Behera, R. K. *Angew. Chem., Int. Ed. Engl.* **1991**, *30*, 1176. (c) Makelburger, H. B.; Jaworek, W.; Vögtle, F. *Angew. Chem., Int. Ed. Engl.* **1992**, *31*, 1571. (d) Issberner, J.; Moors, R.; Vögtle, F. *Angew. Chem., Int. Ed. Engl.* **1994**, *33*, 2413. (e) Alper, J. *Science* **1991**, *251*, 1562. (f) Krohn, K. *Org. Synth. Highlights* **1991**, *378*. (g) Amato, L. *Sci. News* **1990**, *138*, 298. (h) Kim, Y. H.; Webster, O. W. *J. Am. Chem. Soc.* **1990**, *112*, 4592. (i) Hawker, C. J.; Wooley, K. L.; Fréchet, J. M. J. *J. Chem. Soc., Perkin Trans. 1* **1993**, 1287. (j) Fréchet, J. M. J. *Science* **1994**, *263*, 1710.

(2) (a) Tomalia, D. A.; Hall, M.; Hedstrand, D. M. *J. Am. Chem. Soc.* **1987**, *109*, 1601. (b) Tomalia, D. A.; Naylor, A. M.; Goddard, W. A., III. *Angew. Chem., Int. Ed. Engl.* **1990**, *29*, 138. (c) Tomalia, D. A.; Durst, H. D. In *Topics in Current Chemistry*; Weber, E., Ed.; Springer-Verlag: Berlin, Heidelberg, 1993; Vol. 165, p 193.

(3) Duncan, R. *Proc. Natl. Acad. Sci. U.S.A.* **1996**, *93*, 4897.

(4) (a) Bielinska, A.; Kukowska-Latallo, J. F.; Johnson, J.; Tomalia, D. A.; Baker, J. R. *Nucleic Acid Res.* **1996**, *24*, 2176. (b) Kukowska-Latallo, J. F.; Bielinska, A. U.; Johnson, J.; Spindler, R.; Tomalia, D. A.; Baker, J. R., Jr. *Proc. Natl. Acad. Sci.* **1996**, *93*, 4897.

(5) Ottaviani, M. F.; Matteini, P.; Brustolon, M.; Turro, N. J.; Jockusch, S.; Tomalia, D. A. *J. Phys. Chem.* **1998**, *102*, 6029.

(6) *Vesicles*; Surfactant Science Series; Rosoff, M., Ed.; Marcel Dekker: New York, 1996; Vol. 62.

(7) (a) Lasic, D. D. *Liposomes: From Physics to Applications*; Elsevier: Amsterdam, 1993. (b) *Liposomes*; Knight, C. G., Ed.; Elsevier: Amsterdam, 1981. (c) *Liposomes. A Practical Approach*; New, R. R. C., Ed.; Oxford University Press: 1990.

the bulk solution; however, when the exchange rate is decreased, a physical interaction which depends on the dendrimer size (generation) and the protonation of the dendrimer surface groups is evident.<sup>5</sup> Since the labels are attached to the dendrimer in this previous study, no information are obtained concerning eventual modification of the vesicle structure upon interaction with the dendrimers. When a spin label is introduced into the vesicle bilayer or multilayer, EPR techniques can be used to clarify the structure of vesicles both in the absence and in the presence of molecules interacting with them.<sup>11–14</sup> On the other hand, EPR techniques have also been used to investigate interactions of *n*SBDs with surfactant aggregates with embedded probes.<sup>15–17</sup> Mainly, mobility and polarity parameters, other than structural information, may be extracted from the analysis of the CW-EPR spectra of spin probes or spin labels inserted in ordered assemblies, like micelles and vesicles.<sup>18</sup> Conversely, the analysis of the electron spin-echo (ESE) spectra provides information on the structure of the radical environment.<sup>19</sup> Electron spin-echo envelope modulation (ESEEM) studies of phospholipid vesicles with embedded probes have already been shown to provide interesting information on the vesicle structure.<sup>20</sup> Furthermore, ESEEM studies have been carried out to describe the interactions of *n*SBDs with SDS micelles.<sup>21</sup> In the present study, we explore, by both CW-EPR and ESE experiments, the structural modifications of dimyristoylphosphatidylcholine (DMPC) vesicles, which occur upon interaction with the SBDs. The study with labeled dendrimers<sup>5</sup> has demonstrated that these interactions are favored by the so-called higher generation dendrimers ( $G > 4$ ), which possess a more densely packed external topology.<sup>2b,c,22</sup> We selected for this study the  $G = 7$  dendrimer (7SBD), with varied protonation levels of the surface amino groups. Doxylstearic acids with the doxyl group attached at positions 5, 12, and 16 of the stearic chain (termed 5DXSA, 12DXSA, and 16DXSA, respectively) were embedded in the vesicle structure, which allows investigation of structural modifications of the DMPC bilayer when it interacts with the dendrimer,

in comparison to control experiments in the absence of the dendrimer, at various depths from the vesicle surface.

The results obtained from both CW-EPR and ESE experiments on each probe (5DXSA, 12DXSA, and 16DXSA, respectively) are described and discussed separately, since each probe monitors a different region of the phospholipid bilayer. A comprehensive description of the structural modifications of the bilayer, due to the interaction with the dendrimer, is proposed on the basis of these results.

## Experimental Section

The water solutions were prepared in doubly-distilled water filtered through Millipore filters.

DMPC was purchased from SIGMA and used as received. The vesicles were obtained as described by Reeves and Dowben:<sup>23</sup> hydration of the dried lipid film is accomplished by exposing the film to a stream of water-saturated nitrogen, followed by swelling in sucrose solution without shaking. Spinning allows for the removal of floating multilamellar vesicles. Addition of a glucose solution and further spinning produce a pellet of vesicles, which was dissolved in water.

5DXSA, 12DXSA, and 16DXSA were purchased from SIGMA and used as received. A portion of a chloroform (SIGMA) solution of each DXSA, containing 1% in moles of DXSA with respect to the initial amount of DMPC, was first dried and then left equilibrating overnight with the vesicle solution in a nitrogen atmosphere. This procedure was demonstrated, on the basis of previous literature<sup>20,21</sup> and on the basis of the EPR spectral analysis in this work, to favor the insertion of the probe chain in the lipid bilayer. The DMPC-*n*DXSA solutions, both in the absence and in the presence of 7SBD, were used immediately after preparation.

The 7SBD employed in this study has been synthesized as described in previous papers.<sup>2</sup> Careful purification of the dendrimers was accomplished by ultrafiltration at each generational level. The purity was determined by <sup>13</sup>C NMR spectroscopy, mass spectrometry, and gel electrophoresis.<sup>24</sup>

The aqueous 7SBD solution was prepared with the concentration 0.1 M. Unless otherwise specified, the concentration of the SBD solutions is in surface groups. The solutions were stored under nitrogen, to avoid oxidative degradation and kept in the refrigerator when not used. Protonation of the surface amino groups was accomplished by adding controlled amounts of diluted HCl (0.05 M; Merck). The acid-base properties of the SBDs have already been determined in a previous study.<sup>25</sup> The protonated 7SBD (pH = 4.5) will be henceforth termed 7SBD<sup>+</sup>. The dendrimer solutions were then added to the DMPC-*n*DXSA solutions to obtain a final concentration of 0.05 M in surface amino groups.

The EPR spectra were recorded by means of a Bruker 200D spectrometer operating at X band (9.5 GHz), interfaced with Stellar software to a PC-IBM computer for data acquisition and handling. Temperature was controlled with a Bruker ST 100/700 variable-temperature assembly. Unless otherwise specified, the temperature at which the EPR spectra were recorded was 303 K.

Additional experiments were performed as a function of temperature and concentration: (1) temperature variations gave rise to a progressive variation of the correlation time for motion, but the analysis of them did not provide any further information on the system under study, and therefore these measurements are not discussed in the following; (2) variation in the relative concentrations of vesicles, probes, and dendrimers did not produce significant variations in the EPR results, with the exception of probe amounts above 2%, which led to spin-spin interactions in the phospholipid bilayer.

The preparation procedure to provide samples for the ESE measurements was as described above for obtaining the DMPC vesicles + *n*DXSA, the 7SBD, and the dendrimer-vesicle solutions, but with D<sub>2</sub>O (Merck, purity 99.8%) instead of H<sub>2</sub>O.

(8) Fendler, J. H. *Membrane Mimetic Chemistry*; Wiley-Interscience: New York, 1982.

(9) Strom-Jensen, P. R.; Magin, R. L.; Dunn, F. *Biochim. Biophys. Acta* **1984**, *769*, 179.

(10) Maynard, V. M.; Magin, R. L.; Dunn, F. *Chem. Phys. Lipids* **1985**, *37*, 1.

(11) Marsh, D.; Watts, A. In *Liposomes*; Knight, C. G., Ed.; Elsevier: Amsterdam, 1981; p 139. Lasic, D. D. *Bull. Magn. Reson.* **1991**, *13*, 3.

(12) Lasic, D. D. *J. Phys.* **1983**, *44*, 737.

(13) Lomax, T. L.; Mehlhorn, R. J. *Biochim. Biophys. Acta* **1985**, *106*.

(14) (a) Korstanje, L. J.; van Fassen, E. E.; Levine, Y. K. *Biochim. Biophys. Acta* **1989**, *882*, 196. (b) de Jongh, H. H. J.; Hemminga, M. A.; Marsh, D. *Biochim. Biophys. Acta* **1990**, *1024*, 82. (c) Datema, K. P.; Wolfs, C. J. A. M.; Marsh, D.; Watts, A.; Hemminga, M. A. *Biochemistry* **1987**, *26*, 7571.

(15) Ottaviani, M. F.; Cossu, E.; Turro, N. J.; Tomalia, D. A. *J. Am. Chem. Soc.* **1995**, *117*, 4387.

(16) (a) Ottaviani, M. F.; Turro, N. J.; Jockusch, S.; Tomalia, D. A. *J. Phys. Chem.* **1996**, *100*, 13675. (b) Ottaviani, M. F.; Turro, N. J.; Jockusch, S.; Tomalia, D. A. *Colloids Surf.* **1996**, *115*, 9.

(17) Ottaviani, M. F.; Andechaga, P.; Turro, N. J.; Tomalia, D. A. *J. Phys. Chem.* **1997**, *101*, 6057.

(18) (a) *Spin Labeling. Theory and Applications*; Berliner, L. J., Ed.; Academic Press: New York, 1976, Vol. 1; 1979, Vol. 2. (b) *Biological Magnetic Resonance. Spin Labeling. Theory and Applications*; Berliner, L. J., Reuben, J., Eds.; Plenum Press: New York, 1989; Vol. 8.

(19) (a) *Modern Pulsed and Continuous-Wave Electron Spin Resonance*; Kevan, L., Bowman, M. K., Eds.; Wiley-Interscience: New York, 1990. (b) *Time Domain Electron Spin Resonance*; Kevan, L., Schwartz, R., Eds.; Wiley-Interscience: New York, 1979.

(20) (a) Hiromitsu, I.; Kevan, L. *J. Am. Chem. Soc.* **1987**, *109*, 4501. (b) Hiff, T.; Kevan, L. *J. Phys. Chem.* **1989**, *93*, 1572.

(21) Ottaviani, M. F.; Daddi, R.; Brustolon, M.; Turro, N. J.; Tomalia, D. A. *Appl. Magn. Res.* **1997**, *13*, 347.

(22) Naylor, A. M.; Goddard, W. A., III; Kiefer, G. E.; Tomalia, D. A. *J. Am. Chem. Soc.* **1989**, *111*, 2341.

(23) Reeves, J. P.; Dowben, R. M. *J. Cell. Physiol.* **1969**, *73*, 49.

(24) Dvornic, P. R.; Tomalia, D. A. *Macromol. Symp.* **1994**, *88*, 123.

(25) Ottaviani, M. F.; Montalti, F.; Turro, N. J.; Tomalia, D. A. *J. Phys. Chem.* **1996**, *100*, 11033.

The procedure was performed under a nitrogen atmosphere. Deuterated water was used to distinguish modulation due to the deuteria nuclei belonging to the solvent from that due to protons belonging to the dendrimer or the liposome surface, such as the radical backbone.

Quartz EPR tubes were used for the ESE measurements.

The ESE experiments were carried out at 4 K using a Bruker ESP 380E FT-EPR spectrometer equipped with the liquid helium cooling accessory ER4112HV. On the basis of previous literature, we assumed that the structure of dendrimers, liposomes, and their supramolecular arrangements, 7SBD-DMPC, was retained at 4 K, under the conditions of rapid freezing.<sup>20b,26</sup>

Two-pulse (2p) spin-echo signals were registered by varying the time between the pulses. The pulse sequence was (16- $\tau$ -32 ns). The three-pulse (3p) echoes were registered by varying  $T$ , the time between the second and the third pulses. The pulse sequence was (16- $\tau$ -16- $T$ -16 ns). Six modulated echo decays were collected at  $\tau = 160, 168, 176, 184, 192,$  and 200 ns. The magnetic field was set at the central EPR peak, that is, 3487 G.

The ESE spectra of samples containing 7SBD<sup>+</sup> are not reported, since they were very poorly resolved and not informative.

## Results and Discussion

The CW- and pulsed-EPR spectra were analyzed using suitable computer programs.

Computer-aided analysis of the EPR spectra, by means of the well-established procedure developed by Schneider and Freed,<sup>27</sup> provided the following parameters: (a) The correlation time for rotational motion of the nitroxide group,  $\tau$  (the accuracy of  $\tau$ , as obtained from spectral computation, is 5%), assuming a Brownian model for the rotational mobility. The approximation of a Brownian model is supported by the extended use of the same model even for completely ordered materials.<sup>27</sup> The main axis of rotation may change from the usual  $Z$  axis, corresponding to the direction of the  $p$  orbital containing the unpaired electron (which also corresponds to the bilayer axis), to the  $X$  axis, which lays on the N-O bond direction. (b) The principal components of the  $g$  tensor (for the Zeeman coupling between the electron spin and the magnetic field) were assumed to be equivalent to those found for  $n$ DXSA embedded in Langmuir-Blodgett films:<sup>28</sup>  $g_{xx} = 2.0088$ ,  $g_{yy} = 2.0061$ , and  $g_{zz} = 2.0027$ ; the hyperfine  $A$  tensor components (for the coupling between the unpaired electron spin and the nuclear nitrogen spin),  $A_{ij}$ , are obtained from the fitting between the experimental and the computed pattern and provide a measure of the environmental polarity (the accuracy of  $A_{ij}$ , as obtained from spectral computation, is 2%). A decrease in  $\langle A \rangle = (A_{xx} + A_{yy} + A_{zz})/3$  reflects a decrease in the polarity of the radical environment, such as nitroxides inserted in the lipid bilayer. (c) The order parameter,  $S$  (accuracy from calculation is 2%), which measures the wobbling mobility of the radical inserted in an ordered structure, such as surfactant chains structured in a bidimensional array. (d) The partition of the probes in different environments, when the exchange is slow in the EPR time scale, gave rise to the superposition of different signals to constitute the overall EPR line shape. A subtraction procedure of the computed components from the experimental signal, together with an addition subtraction of the computed components to reproduce the experimental signal, allowed the extraction of the parameters of each component and

the different percentages of the components. The precision in the parameters decreased for more than two components.

The fitting of each EPR signal—by changing as many parameters as the number of  $A_{ij}$  components (to account for polarity variations from external to internal vesicle structure), the order parameter (to account for insertion of the probe in the ordered phospholipid structure), and the correlation time for motion (to account for decreasing microviscosity, mainly due to vesicle-dendrimer interactions) with, if necessary, a tilt of the main rotational axis—may be questionable. Anyway, it is well-known<sup>27</sup> that each parameter differently affects the EPR line shape. Therefore, we have performed an extended analysis of the spectra by changing each parameter and fixing each value in correspondence with the best fitting between the experimental and the computed line shapes. Of course, we cannot exclude that a different set of parameters may reproduce a similar fitting for each spectrum, but the high accuracy in the performed analysis is in favor of the choice of the parameters reported in the tables.

The ESE spectra simulation method has been described by Romanelli and Kevan.<sup>29</sup> Both the two-pulse ( $\pi/2-\tau-\pi$ ) Hahn echo and the three-pulse ( $\pi/2-\tau-\pi/2-T-\pi/2$ ) stimulated echo were recorded and analyzed.

The modulated decay curve in both 2p- and 3p-ESE experiments is described by the function<sup>30</sup>  $V(t) = V_m(t) V_d(t)$ , where  $V_m(t)$  describes the modulation pattern at the ENDOR frequencies  $\nu_+$  and  $\nu_-$  (for the 2p-ESE experiment, modulation also occurs at  $\nu_+ \pm \nu_-$ ) and  $V_d(t)$  is the decay function (the decay of the echo is observed on varying the time interval between the first two pulses and that between the second and the third pulses, for the 2p-ESE and the 3p-ESE experiments, respectively).

Analysis of the modulation pattern is based on the assumption of isotropic shells with weakly coupled nuclei around the electron spin distribution at distances below 0.6 nm. This simulation is performed with a best fit procedure in which the parameters are the type and number  $n^0_i$  of nuclei inducing modulation, their distance from the paramagnetic center  $r_i$  (the accuracy of  $r_i$ , as obtained from computation, is 0.005 nm), and their hyperfine coupling constants  $a_i$  (the accuracy of  $a_i$ , as obtained from computation, is 0.02 MHz). In the case of deuterium, the modulation function  $V_m(t)$  was computed by means of the second-order perturbation approach derived by Heming et al.<sup>31</sup>

In the case of the 3p-ESE experiment, for a pair of values of  $\nu_{\pm}$  and  $\tau$  (the time interval between the two first pulses) such that  $\nu_{\pm}\tau = n$ , where  $n$  is an integer, the modulation at the corresponding frequency disappears.<sup>32</sup> To avoid the latter "blind spots", we have collected a series of six echo decays varying between 160 and 200 ns.

The modulation pattern is not affected by the protons of the methyl groups attached to the piperidine ring. In fact, the modulation depth in ESEEM spectra for each coupled nucleus depends on the anisotropy of the corre-

(29) Romanelli, M.; Kevan, L. *J. Magn. Reson.* **1991**, *91*, 549.

(30) (a) Kevan, L. In *Time Domain Electron Spin Resonance*; Kevan, L., Schwartz, R., Eds.; Wiley-Interscience: New York, 1979; Chapter 8. (b) Salikhov, K. M.; Tsvetkov, Yu. D. In *Time Domain Electron Spin Resonance*; Kevan, L., Schwartz, R., Eds.; Wiley-Interscience: New York, 1979; Chapter 7. (c) Brown, I. M. In *Time Domain Electron Spin Resonance*; Kevan, L., Schwartz, R., Eds.; Wiley-Interscience: New York, 1979; Chapter 6. (d) Mims, W. B. *Phys. Rev.* **1968**, *168*, 370.

(31) Heming, M.; Narayana, M.; Kevan, L. *J. Chem. Phys.* **1985**, *83*, 1478.

(32) Schweiger, A. *Modern Pulsed and Continuous-Wave Electron Spin Resonance*; Kevan, L., Bowman, M. K., Eds.; Wiley: New York, 1990.

(26) (a) Hashimoto, S.; Thomas, J. K. *J. Am. Chem. Soc.* **1983**, *105*, 5230. (b) Baglioni, P.; Kevan, L. *J. Phys. Chem.* **1987**, *91*, 1516.

(27) Schneider, D. J.; Freed, J. H. In *Biological Magnetic Resonance. Spin Labeling. Theory and Applications*; Berliner, L. J., Reuben, J., Eds.; Plenum Press: New York, 1989; Vol. 8, p 1.

(28) Bonosi, F.; Gabrielli, G.; Martini, G.; Ottaviani, M. F. *Langmuir* **1989**, *5*, 1037.

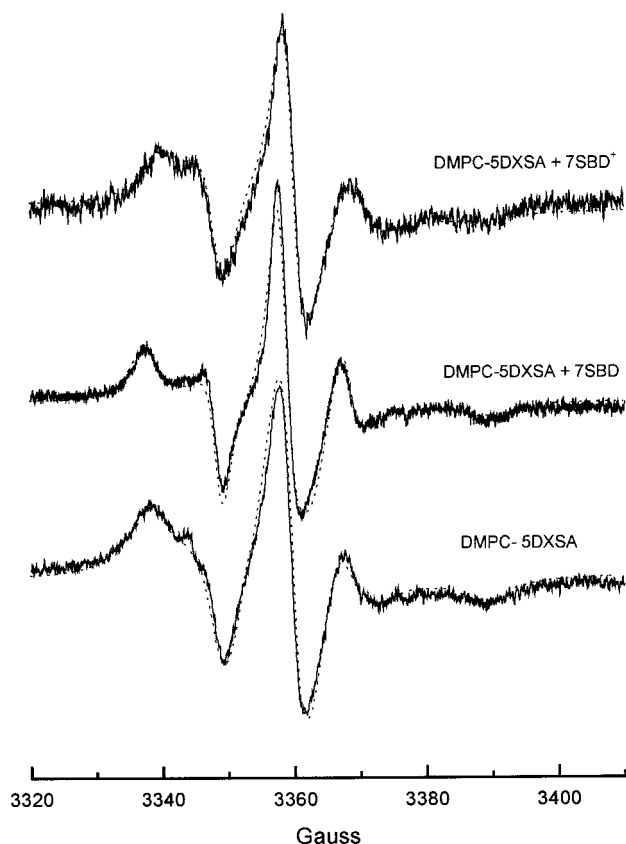


**Figure 1.** Experimental (full lines, 303 K) and computed (dashed lines) EPR spectra of DMPC vesicles containing 1% 5DXSA in the absence and in the presence of 7SBD and 7SBD<sup>+</sup>.

sponding hyperfine tensor,<sup>33</sup> which, for the methyl groups, is averaged by rotation. In fact it has been reported that the methyl group rotation of methyl-substituted benzenes is quite fast ( $3 \times 10^{-5}$  s) even at 2 K.<sup>34</sup>

The decay function  $V_d(t)$  is affected by the concentration  $C_a$  of the spins at resonance (the accuracy of  $C_a$ , as obtained from calculation, is 5%). For nitroxide radicals at low temperature it has been shown that the decay time depends on the modulation of the hyperfine interactions of the unpaired electron spin with the rotating methyl groups of the radical itself.<sup>35</sup> Therefore, the decay time obtained from computation directly provides the correlation time for the methyl groups rotation,  $t_c$  (the accuracy of  $t_c$ , as obtained from calculation, is 10%).

The reliability of the parameters, reported and discussed in the following text, is ensured by the reproducibility of the EPR and ESE spectra, by repeating preparations of the samples, and by the oneness of the set of parameters which fit every experimental signal.

**DMPC-5DXSA System.** Figure 1 shows the experimental (full lines, 303 K) and the computed (dashed lines) EPR spectra of DMPC vesicles containing 1% 5DXSA in the absence and in the presence of 7SBD and 7SBD<sup>+</sup>. The main parameters used for the computation are reported in Table 1.

In the absence of the SBD molecules, the doxyl group is partially inserted in the lipid bilayer, on the basis of the following results: (i) The environmental polarity slightly diminishes with respect to that of the radical in water; that is, the  $A_{ij}$  values are lower than those found for the

**Table 1. Main Parameters for the Computation of the EPR Spectra of DMPC Vesicles Containing 1% nDXSA, in the Absence and in the Presence of nSBDs**

probe	SBD	$A_{xx}^a$ (G)	$A_{yy}^a$ (G)	$A_{zz}^a$ (G)	$\tau^b$ ( $\times 10^{-9}$ s)	$S^c$
5DXSA	no	5.0	6.0	34.0	6.0	
5DXSA	7SBD	5.5	6.0	32.0	3.5	0.53
5DXSA	7SBD <sup>+</sup>	5.0	5.0	35.0	1.5	0.38
12DXSA	no	5.0	5.0	32.0	4.0	0.22
12DXSA	7SBD	5.0	5.0	32.0	4.5 <sub>rot axis X-Z</sub>	0.38
12DXSA	7SBD <sup>+</sup>	5.0	5.0	32.0	2.5	
16DXSA	all samples	5.0	5.0	32.0	1.25	
"vesicular"						
16DXSA "free"	15% no, 20% 7SBD	6.0	6.0	35.6	0.1	
16DXSA	water	6.0	6.0	35.5	0.05	

<sup>a</sup> Accuracy of  $A_{ij}$ : 2%. <sup>b</sup> Accuracy of  $\tau$ : 5%. <sup>c</sup> Accuracy of  $S$ : 2%.

radical in water (the same as reported in Table 1 for 16DXSA in water). (ii) The rotational mobility decreased; that is,  $\tau$  increased, if compared to that of the radical in water ( $\tau = 5 \times 10^{-11}$  s).

The addition of 7SBD to the DMPC-5DXSA system affected the structure of the bilayer in the region containing the doxyl group, on the basis of the following results: (i) A partial ordering of the probe + phospholipid chains occurred by adding 7SBD; that is, the computation needed  $S = 0.53$ , whereas, in the absence of SBDs, no order parameter was required for computing the spectrum. (ii) The environmental polarity further decreased (decrease in  $A_{ij}$ ). (iii) The rotational mobility increased (decrease in  $\tau$ ); that is, despite the ordering of the chains, the nitroxide group increased the freedom of rotational motion. A recent study<sup>5</sup> has shown that the interaction between dendrimer and DMPC vesicles compresses the water layer at the interphase, leading to a higher hydration of the polar heads. This well accounts for the increased rotational mobility of the doxyl group in the vicinity of the head layer. The ESE results supported this finding (see below).

It is of interest that the computational parameters for DMPC-5DXSA + 7SBD were almost equivalent to those reported for 5DXSA in SDS micelles interacting with SBDs.<sup>21</sup> In the latter case it was hypothesized that the micellar structure was modified toward an elongated double-layer structure. Therefore, it is not surprising that the lipid chain organization in the region in the vicinity of the polar heads is similar for such structurally modified micelles and the vesicles upon interaction with the SBD surface.

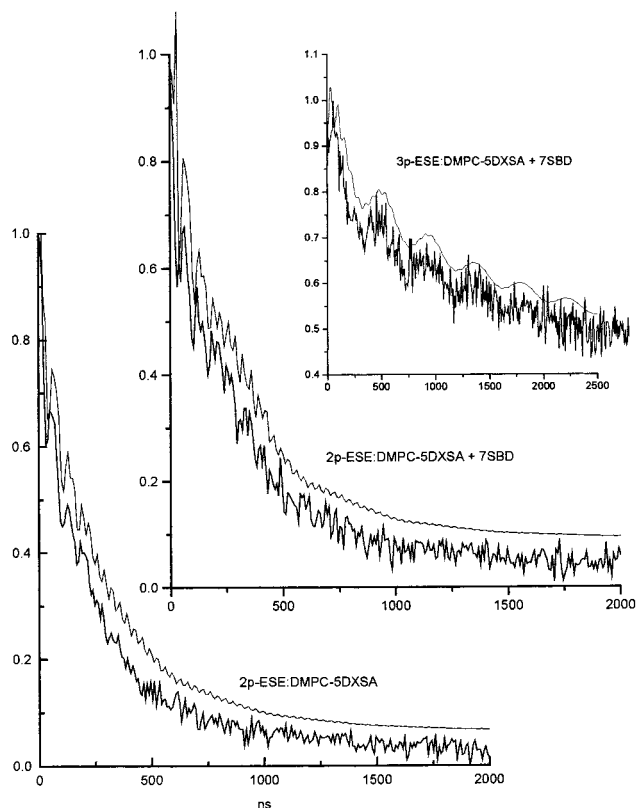
The protonation of the dendrimers caused the decrease of both  $\tau$  and  $S$ , whereas the  $A_{ij}$  values increased, with respect to those for unprotonated dendrimers. It has been reported that the phospholipid bilayer structure of the vesicles partially swells when interacting with acid species.<sup>6,7</sup> The swelling of the vesicle structure when interacting with 7SBD<sup>+</sup> accounted well for the variation of the parameters with respect to those for interaction with unprotonated dendrimers, that is (i) the decrease of the ordering of the interacting bilayer, (ii) the increased rotational mobility, and (iii) the increased environmental polarity.

Figure 2 shows the 2p-ESE spectra of DMPC vesicles containing 1% 5DXSA in the absence and in the presence of 7SBD. The top inset shows the 3p-ESE spectrum of the DMPC-5DXSA + 7SBD system (for simplicity the 3p-ESE spectrum of the DMPC-5DXSA system is not reported). The thick lines (bottom curves) are the experimental spectra (4 K); the thin lines over the experimental spectra are the computed spectra. The main parameters, which gave a good fitting for both the 2p- and the 3p-

(33) Mims, W. B. *Phys. Rev. B* **1972**, *5*, 2409.

(34) Allen, P. S.; Cowking, A. *J. Chem. Phys.* **1968**, *49*, 789.

(35) Romanelli, M.; Martini, G.; Ristori, S.; Kevan, L. *Colloids Surf.* **1990**, *45*, 145.



**Figure 2.** 2p-ESE spectra of DMPC vesicles containing 1% 5DXSA in the absence and in the presence of 7SBD, and 3p-ESE spectrum of the DMPC-5DXSA + 7SBD system: thick lines (bottom lines in each graph), experimental spectra (4 K); thin lines over the experimental spectra, computed spectra.

**Table 2. Main Parameters for the Computation of the Modulation (a) and the Decay pattern (b) of the ESE Signal of DMPC Vesicles Containing 1% *n*DXSA in the Absence and in the Presence of 7SBD**

(a) Modulation								
probe	SBD	no. of H	$r_1^a$ (nm)	$a_1^a$ (MHz)	no. of $D_1$	$r_2^a$ (nm)	no. of $D_2$	$r_3^a$ (nm)
5DXSA	no	6	0.30	-0.1	1	0.36		
5DXSA	7SBD	6	0.30	-0.1	1	0.33		
12DXSA	no	6	0.30	-0.1				
12DXSA	7SBD	6	0.27	-0.2				
16DXSA	no	85%	6	0.31	-0.1			
		15%			2	0.23 <sup>b</sup>	2	0.34
16DXSA	7SBD	80%	6	0.31	-0.1			
		20%			2	0.23 <sup>b</sup>	2	0.34
(b) Decay Pattern								
sonda	SBD	$\tau_c^c$ ( $\mu$ s)	$C_a^d$ ( $\times 10^{-4}$ mol/L)					
5DXSA	no	0.3	8.5					
5DXSA	7SBD	0.3	7.0					
12DXSA	no	0.1	4.0					
12DXSA	7SBD	0.5	8.0					
16DXSA	no, 7SBD	0.3	4.0					

<sup>a</sup> Accuracy of  $r_i$  and  $a_i$ : 2%. <sup>b</sup>  $a_1 = 0.3$  MHz and  $Q_1$  (quadrupole constant) = 0.4 MHz were introduced in the calculation. <sup>c</sup> Accuracy of  $\tau_c$ : 10%. <sup>d</sup> Accuracy of  $C_a$ : 5%.

patterns, are reported in Table 2a, for the calculation of the modulation pattern (ESEEM), and Table 2b for the decay pattern calculation. The main findings on the basis of the analysis of the parameters are as follows:

(1) The accuracy in the parameters for the proton modulation is quite low due to the noise in the experimental spectra. In any case, six protons fit the modulation well at a distance of 0.3 nm. These protons do not belong

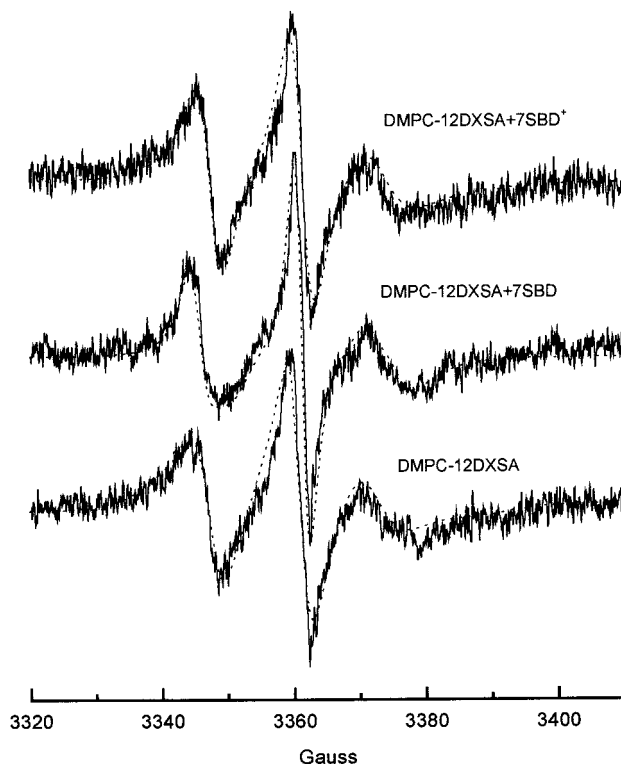


**Figure 3.** Experimental (full lines, 303 K) and computed (dashed lines) EPR spectra of DMPC vesicles containing 1% 12DXSA in the absence and in the presence of 7SBD and 7SBD<sup>+</sup>.

to the nitroxide group for the following reasons: (i) The rotation of the methyl groups of the radical at 4 K induces the averaging of the dipolar component of the hyperfine coupling of the methyl groups themselves. Consequently, the methyl groups of the nitroxide do not participate in the echo modulation. (ii) The distance between the protons of the methylene group of the doxyl ring and the N-O group is 0.35 nm,<sup>36</sup> which is larger than the proton distance calculated from computation (0.3 nm). Therefore, the protons responsible for the modulation pattern belonged to the methylene groups of the carbon chains of both the probe and the phospholipid in the vicinity of the N-O moiety.

(2) In the absence of 7SBD a modulation due to deuterium nuclei was poorly recognizable in the 2p-ESE signal, for two main reasons: (i) only one deuterium, not complexed ( $a_{iso} = 0$ ) and quite far from the N-O moiety ( $r = 0.36$  nm), gave rise to the modulation pattern; (ii) the decay was fast, mainly due to a high  $C_a$  concentration. These results indicated low water permeability in the region occupied by the doxyl group.

(3) The addition of 7SBD caused two main variations in the parameters in Table 2; that is, (i) the deuterium atom comes closer to the N-O group ( $r = 0.33$ ), and (ii) the  $C_a$  concentration decreases. Again, these findings indicate an increased water permeability (in the region of the doxyl group), upon interaction with the dendrimer. The EPR and the ESE results, therefore, support each other in describing the structural variation of the vesicle bilayer by addition of the dendrimer.

**DMPC-12DXSA System.** Figure 3 shows the experimental (full lines, 303 K) and the computed (dashed lines) EPR spectra of DMPC vesicles containing 1% 12DXSA in

(36) Dikanov, S. A.; Shubin, A. A.; Parmon, V. N. *J. Magn. Reson.* **1981**, *42*, 474.

the absence and in the presence of 7SBD and 7SBD<sup>+</sup>. The main parameters used for the computation are reported in Table 1.

Conversely to the DMPC–5DXSA sample, the DMPC–12DXSA sample in the absence of the dendrimers already shows a partial ordering of the chains ( $S = 0.22$ ), and the rotational mobility is still slow but faster than that for the 5DXSA sample. Furthermore, the environmental polarity (tested by the  $A_{ij}$  values) is as low as expected for the radical inserted in the lipid core of the bilayer. We may deduce that the stearic chain is embedded and ordered into the lipid bilayer in the region of quite high fluidity, corresponding to C10–C12 of the carbon chain of the phospholipid.<sup>6,7</sup>

The addition of 7SBD also caused variations of the bilayer structure, but ones that were in part different with respect to those in the region of the bilayer probed by 5DXSA. The variations are as follows: (i) The order increased ( $S = 0.38$ ), as found with 5DXSA, but to a lower extent. (ii) The rotational mobility remained almost unchanged, but a tilting of the main rotational axis from the  $Z$  axis toward the  $X$  axis (about  $50^\circ$ ) was requested for the fitting. A tilting of the chains is described in the literature<sup>6,7</sup> for phospholipid membranes in the transition from liquid-crystalline phase to the phase, corresponding to a transition from the so-called gauche conformation to the trans conformation giving rise to a more highly packed structure. The tilt is quantified as  $58^\circ$  and is in good agreement with the tilting obtained from this EPR analysis. We suppose that the interaction of the vesicle surface with the dendrimer partially rigidifies the bilayer structure as obtained below the liquid-crystalline–gel transition.

As found for 5DXSA samples, the addition of the protonated dendrimer 7SBD<sup>+</sup> caused a disordering of the chains and an increase in the rotational mobility, probably due to the swelling of the vesicle upon interaction with acid species.

Figure 4 shows the 2p-ESE spectra of DMPC vesicles containing 1% 12DXSA in the absence and in the presence of 7SBD. The thick lines (bottom curves) are the experimental spectra (4 K); the thin lines over the experimental spectra are the computed spectra. The main parameters from computation are reported in Table 2a, for the calculation of the modulation pattern (ESEEM), and Table 2b, for the decay pattern calculation. The 3p-ESE spectra are not reported, since they were very poorly defined: no modulation was recognizable, and the decay pattern was computed with the same parameters obtained for the 2p-ESE spectra. The main findings on the basis of the analysis of the parameters are as follows:

(1) No modulation due to coupling of the unpaired electron with the deuterium atoms was found, since the deuterated water could not penetrate into the bulk of the lipid bilayer, where the doxyl is located.

(2) The small but not negligible decrease in distance of the protons, which gave rise to the modulation, probably arose from methylene groups belonging to the carbon chains of neighboring phospholipids. This means that these lipid chains came a little bit closer to the doxyl group.

(3) The decay of the ESE signal of 12DXSA samples in the absence of the dendrimer is slower than that found for 5DXSA samples: the faster proton mobility ( $\tau_c = 0.1 \mu\text{s}$ ) and the lower spin concentration suggested a lower packing of the chains and are expected for the increased fluidity of the bilayer region at position 12 of the carbon chains.

(4) The decay in the presence of 7SBD is much faster than that in the absence of the dendrimer, since both the

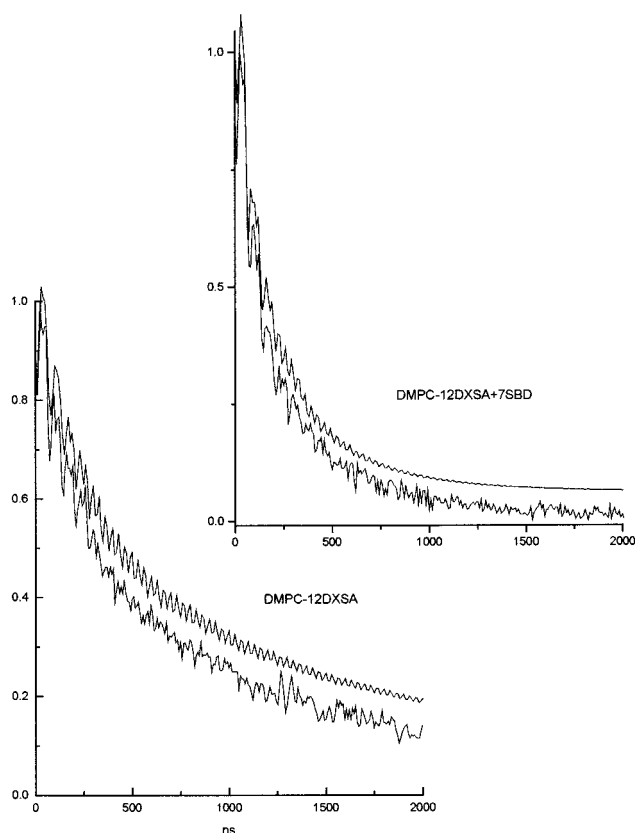


**Figure 4.** 2p-ESE spectra of DMPC vesicles containing 1% 12DXSA in the absence and in the presence of 7SBD: thick lines (bottom lines in each graph), experimental spectra (4 K); thin lines over the experimental spectra, computed spectra.

proton mobility decreased (increase of  $\tau_c = 0.5 \mu\text{s}$ ) and the spin concentration increased. These findings confirmed the results obtained by CW-EPR; that is, the bilayer becomes more rigid upon interaction between the vesicle and the dendrimer, and, as also as indicated the literature,<sup>6,7</sup> the chains of adjacent phospholipid molecules (the stearic chain followed the same fate) are in closer proximity.

**DMPC–16DXSA System.** Figure 5 shows the experimental EPR spectra (full lines, 303 K) of DMPC vesicles containing 1% 16DXSA in the absence and in the presence of 7SBD and 7SBD<sup>+</sup>. The spectra consist of two components. The subtraction–addition procedure of the experimental and computed signals allows the separation, quantification, and analysis of each component. In Figure 5 the so-called “free” and “vesicular” computed components are shown as dotted and dashed lines, respectively. The main parameters used for the computation of the two components are reported in Table 1, together with the parameters for the computation of the spectrum of 16DXSA in water (not reported) at the same temperature.

The parameters used for the computation of the two components were the same in the absence and in the presence of the dendrimers. Only the relative percentages of the two components changed slightly. The “vesicular” component, which was predominant both in the absence and in the presence of the dendrimer, was computed with the same  $A_{ij}$  components as used for 12DXSA samples. This indicated insertion of the probes into the bilayer structure, with the doxyl group embedded in the lipid region. Position 16, at the end of the stearic chain, corresponded to the localization of the doxyl group between the two layers constituting the phospholipid bilayer, in a region which is characterized by high fluidity and complete

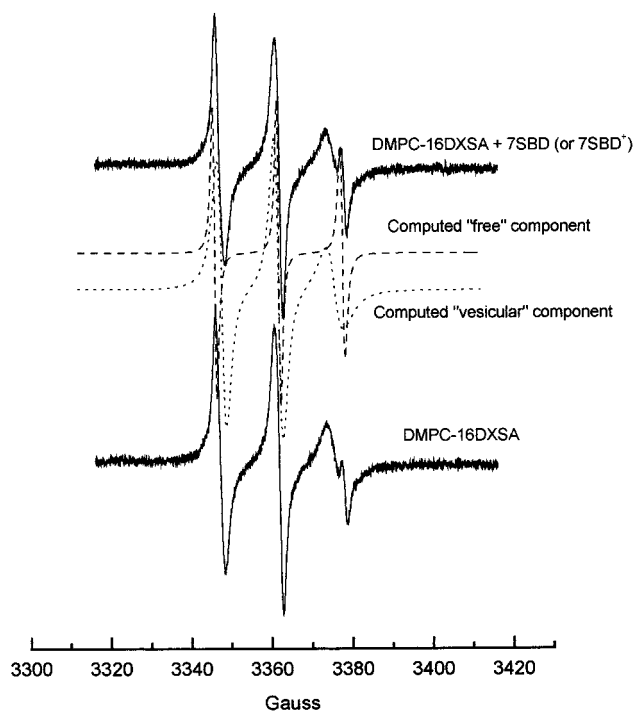


**Figure 5.** Experimental EPR spectra (full lines, 303 K) of DMPC vesicles containing 1% 16DXSA in the absence and in the presence of 7SBD and 7SBD<sup>+</sup>. The “free” and “vesicular” computed components are shown as dotted and dashed lines, respectively.

disorder.<sup>6,7</sup> This localization was confirmed by the spectral parameters, that is, a rotational mobility at the lower limit of the so-called slow motion condition ( $\tau \sim 1 \times 10^{-9}$  s) and  $S = 0$ .

The  $A_{ij}$  components of the “free” signal were the same as those for 16DXSA in water. Two main hypotheses may be suggested for the localization of this small fraction of 16DXSA: (i) nonadsorbed by the vesicle and free in solution; (ii) adsorbed by the vesicle in a U(bent)-conformation, which allows for both the polar groups to hydrate at the vesicle/water interface, whereas the stearic chain is embedded in the lipid region. In both cases, high rotational mobility and high environmental polarity are expected. The following experimental data support the second hypothesis: (i) Hiff and Kevan have found by ESE analysis a U-conformation for 16DXSA in phospholipid bilayers;<sup>20b</sup> (ii) the rotational mobility evaluated for the “free” 16DXSA was half of that found for 16DXSA in water (Table 1). The small increase of the percentage of the “free” component upon addition of the dendrimer indicated that a larger portion of radical was forced to the U-conformation to promote the interaction of the polar doxyl group with the polar surface of the dendrimer.

Figure 6 shows the 2p-ESE spectra of DMPC vesicles containing 1% 16DXSA in the absence and in the presence of 7SBD. The top inset shows the 3p-ESE spectrum of the DMPC-16DXSA + 7SBD system (for simplicity the 3p-ESE spectrum of the DMPC-5DXSA system is not reported). The thick lines (bottom curves) are the experimental spectra (4 K); the thin lines over the experimental spectra are the computed spectra. The main parameters, which gave a good fit for both the 2p and the 3p patterns, are reported in Table 2a, for the calculation of the modulation pattern (ESEEM), and Table 2b for the calculation of the decay pattern.

Analysis of the ESE spectra by best fit calculations was performed on the basis of the EPR spectra. For the analysis

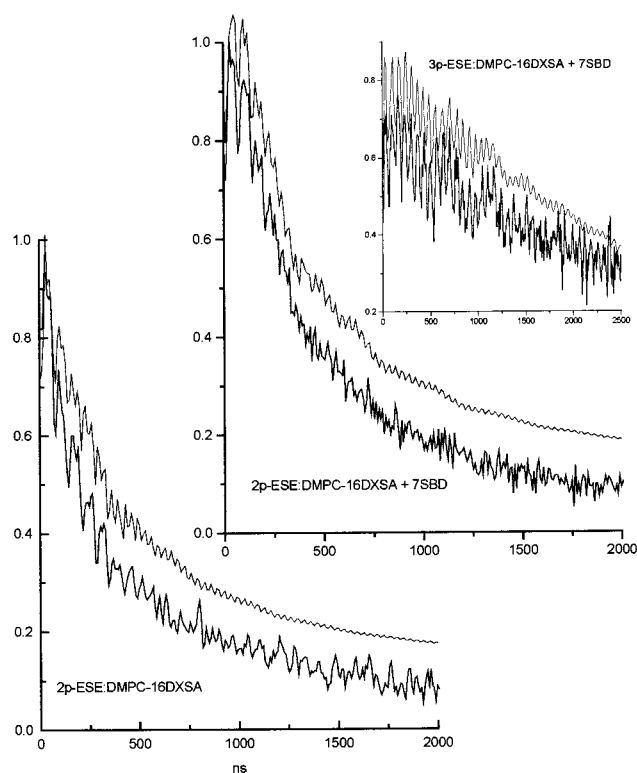


**Figure 6.** 2p-ESE spectra of DMPC vesicles containing 1% 16DXSA in the absence and in the presence of 7SBD, and 3p-ESE spectrum of the DMPC-16DXSA + 7SBD system: thick lines (bottom lines in each graph), experimental spectra (4 K); thin lines over the experimental spectra, computed spectra.

we assumed the following: (i) as for the EPR spectra, two components constituted the ESE signals, and the percentage of the “free” component increased from 15% to 20% upon addition of the dendrimer to the DMPC-16DXSA solution; (ii) the “vesicular” component does not show any modulation of deuterium nuclei, since the doxyl is completely embedded in the lipid bilayer; (iii) the “free” component does not show any modulation of proton nuclei, since the doxyl is completely exposed to the external deuterated water (This assumption is clearly an oversimplification; however, it worked in the calculation.); (iv) the same decay was assumed for the two components. (Of course, we also expect that this assumption is an oversimplification, but it was necessary since the decay contribution arising from each component could not be quantified.)

The analysis was carried out by computing the vesicular component for the proton modulation, and then, by subtraction of this component at the proper percentage, the free component was calculated. The following information is obtained by analysis of the parameters in Table 2a: (i) again six protons, at about the same distance as found for the other probes, gave rise to the modulation of the ESE signal; (ii) two shells of deuteria, composed each of two deuteria, accounted for the modulation due to the coupling of deuterium nuclei with the unpaired electron; the closest shell ( $r = 0.23$  nm) also showed  $a_{\text{iso}} = 0.3$  MHz. Two deuterium atoms were therefore complexed by the N-O moiety. Conversely, the other two deuterium atoms were quite far from the paramagnetic center ( $r = 0.34$  nm) and not complexed by it. In conclusion, two water molecules were identified in the vicinity of the doxyl group belonging to the 16DXSA molecules in the bent conformation.

### Conclusion: Structural Modifications of the DMPC Vesicles upon Interaction with SBD Molecules

Information on the bilayer structure, as obtained by the use of DXSA spin probes embedded into the phospholipid bilayer structure, from the EPR and ESE techniques, is as follows:

**1. Ordering of the Bilayer.** (i) The ordering increases in the presence of the dendrimer. (ii) In the absence of the dendrimer, the ordering in the region close to the polar heads is probably perturbed by the doxyl group, which weakly interacted with the polar heads. The ordering was higher in the central region of the layer and then diminished going to the end of the chains. (iii) In the presence of the dendrimer, the ordering decreased from the region in the vicinity of the polar heads to the end of the chain.

**2. Rotational Mobility of the Chains.** (i) Slow motion conditions ( $1 \times 10^{-9} \text{ s} < \tau < 5 \times 10^{-8} \text{ s}$ ) were found for the *n*DXSA embedded in the phospholipid bilayer. (ii) In the absence of the dendrimer, the mobility decreased from the region in the vicinity of the polar heads to the end of the chains. (iii) In the presence of the dendrimer, the mobility increased in the region close to the polar heads, probably due to the compression of the water layers at the interphase,<sup>5</sup> which increased the water permeability in that region. The rotational mobility in the rest of the chain was essentially unchanged.

**3. Tilting of the Chains.** In line with the increased ordering, the structure of the bilayer became more rigid (comparable to gel conditions) due to the interaction with the dendrimer, which promoted a tilting of the chains, mainly evident in the central region of the phospholipid layer.

**4. Polarity of the Doxyl Environment.** (i) The polarity in the region close to the polar heads was affected by the interaction between the doxyl groups and the polar heads themselves but diminished upon addition of the

dendrimers, because of the interaction of the polar heads with the dendrimer surface and the consequent quenching (ordering) of the structure. (ii) Low environmental polarity was found for the doxyl groups in the layer regions far from the polar heads.

**5. Permeability to Water.** the permeability to water was quite low even in the vicinity of the polar heads in the absence of the dendrimers but increased in that region upon addition of the dendrimer, due to the compression of the water layer at the interface.

**6. Swelling of the Bilayer upon Interaction with Protonated Dendrimers.** The addition of the protonated dendrimers had a similar effect to that from the addition of acid species; that is, the chain packing and the ordering of the chains diminished due to the swelling of the bilayer.

In summary, the results obtained in this study indicate that the bilayer structure is modified but only partially perturbed by addition of the dendrimers, and the integrity of the vesicle, as a model cell membrane, is preserved after the interaction with the dendrimers. This is further encouragement for the use of the SBDs as gene and drug carriers.

Further studies are in progress, using other probes and other kinds of phospholipids. Also, this study will continue by analyzing the interactions with proteins, as membrane components, and with DNA and oligonucleotides.

**Acknowledgment.** The authors are very grateful to Prof. M. Romanelli for providing programs to compute the ESE patterns. N.J.T. thanks the NSF and NATO for their generous support. D.A.T. thanks the Army Research Laboratory (ARL/MMI Dendrites Poly-Center of Excellence) and Dendritech Inc. for generous support and for certain critical synthetic efforts. M.F.O. and R.D. thank the Italian Ministero Università e Ricerca Scientifica e Tecnologica (MURST) for financial support.

LA9803068